Article

Smectic Liquid Crystals from Supramolecular Guanidinium Alkanesulfonates

Fabrice Mathevet, Patrick Masson, Jean-Franois Nicoud, and Antoine Skoulios

J. Am. Chem. Soc., **2005**, 127 (25), 9053-9061• DOI: 10.1021/ja051312a • Publication Date (Web): 02 June 2005

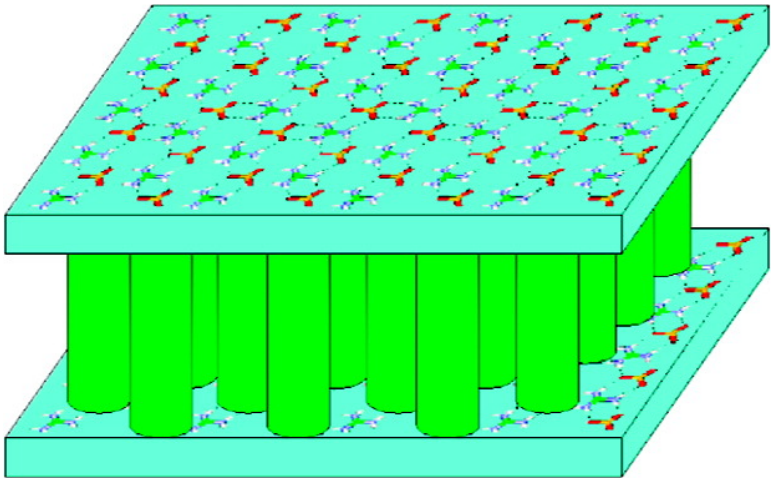

J|A|C|S
ARTICLES
Published on Web 06/02/2005

Smectic Liquid Crystals from Supramolecular Guanidinium Alkanesulfonates†

Fabrice Mathevet, Patrick Masson,* Jean-François Nicoud, and Antoine Skoulios

Contribution from the Institut de Physique et Chimie des Matériaux de Strasbourg, Groupe des Matériaux Organiques (CNRS UMR 7504), Université Louis Pasteur, 23 rue du Loess, 67034 Strasbourg Cedex 2, France

Received March 2, 2005; E-mail: patrick.masson@ipcms.u-strasbg.fr

Abstract: The thermotropic polymorphism of a series of guanidinium alkanesulfonates ($6 \leq n \leq 18$) was investigated by optical microscopy and differential scanning calorimetry. Hydrogen bonding was analyzed by infrared spectroscopy. Molecular volumes were measured by dilatometry. The structure of the crystal, smectic A, and *ordered* smectic phases observed were studied by X-ray diffraction and utilized to prove that the supramolecular arrangement of the molecules in the crystal survives in the smectic phases at high temperature.

Introduction

The crystal structure of a variety of organic derivatives of guanidinium sulfonate was studied recently by X-ray diffraction.[1] Of lamellar symmetry, the structures were found to consist of two types of layers alternately superposed in a periodic fashion, one made of the ionic groups, the other of the organic residues of the molecules. Strongly interacting through Coulombic forces and hydrogen bonding, in accordance with the concepts of supramolecular chemistry,[2] the guanidinium and sulfonate ions self-assemble into well-defined two-dimensional honeycomb networks. Covered only on one side when the organic residues are thin, the supramolecular ionic sheets are associated in pairs by bracketing together their polar surfaces. Applying to the case of guanidinium ethanesulfonate taken as an example, Figure 1 shows the double-layered arrangement of the ionic species and the interdigitated packing of the thin organic residues in the crystals.

In a subsequent work, a series of long-chained guanidinium alkylbenzenesulfonates (noted as GABS-*n*) were studied as a function of increasing temperature with a variety of experimental techniques.[3] Just as expected from the area covered by the sulfonic groups in the honeycomb networks (about 45 Å^2), a sufficiently large area to let the alkyl chains (whose cross-sectional area is of 18.5 Å^2)[4] melt without disturbing the lamellar packing of the molecules, the GABS-*n* compounds were found to produce smectic A phases at high temperature, that is, lamellar arrangements of molecules laterally packed in a liquidlike fashion.[5,6] Despite the short-ranged ordering of the ions and alkyl chains inside the layers, the honeycomb supramolecular architecture observed in the crystal at room temperature seems, as indicated by infrared spectroscopy, to survive almost undamaged in the smectic phases at high temperature. This possibility of getting smectic phases with the GABS-*n* compounds was immediately confirmed in an independent work and further generalized to the related alkylbiphenylsulfonate derivatives of guanidinium.[7]

In the present work, the homologous series of guanidinium alkanesulfonates (noted as GAS-*n*, $6 \leq n \leq 18$) was synthesized and studied as a function of temperature with a variety of experimental techniques:

$$H(CH_2)_n-SO_3^{\ominus} \quad C(NH_2)_3^{\oplus}$$

It was expected to get not only smectic A but also *ordered* smectic phases, in the layers of which the molecules are laterally arranged in an orderly fashion, according to well-defined two-dimensional crystal lattices (hexagonal for smectic B,[6,8,9] centered rectangular for smectic E,[6,10] and tetragonal for smectic T[11,12]). The in-layer structure of such *ordered* smectic phases should, of course, be liable to provide explicit evidence of any supramolecular architecture surviving at high temperature. Contrary to the GABS-*n* compounds, where the electric charge of the sulfonic groups is partially delocalized over the benzene

† The present article is part of the Ph.D. dissertation work defended by one of us (F.M.) at the Louis-Pasteur University of Strasbourg on December 20, 2002.

(1) Russell, V. A.; Etter, M. C.; Ward, M. D. *J. Am. Chem. Soc.* **1994**, *116*, 1941−1952.
(2) Lehn, J. M. *Supramolecular Chemistry: Concepts and Perspectives*, VCH: Weinheim, Germany, 1995.
(3) Mathevet, F.; Masson, P.; Nicoud, J.-F.; Skoulios, A. *Chem.—Eur. J.* **2002**, *8*, 2248−2254.
(4) Kitaigorodskii, A. I. *Organic Chemical Crystallography*; Consultant Bureau: New York, 1961; p 180.
(5) Skoulios, A.; Luzzati, V. *Nature* **1959**, *183*, 1310−1312.
(6) Goodby, J. W. In *Handbook of Liquid Crystals, Low Molecular Weight Liquid Crystals I*; Demus, D., Goodby, J., Gray, G.W., Spiess, H.W., Vill, V., Eds.; Wiley-VCH: Weinheim, Germany, 1998; Vol. 2A, pp 3−21.
(7) Martin, S. M.; Yonezawa, J.; Horner, M. J.; Macosko, C. W.; Ward, M. D. *Chem. Mater.* **2004**, *16*, 3045−3055.
(8) de Gennes, P. G.; Prost, J. *The Physics of Liquid Crystals*; Clarendon Press: Oxford, 1993.
(9) Gallot, B.; Skoulios, A. *Mol. Cryst.* **1966**, *1*, 263−292.
(10) Vincent, J. M.; Skoulios, A. *Acta Crystallogr.* **1966**, *20*, 441−447.
(11) Alami, E.; Levy, H.; Zana, R.; Weber, P.; Skoulios, A. *Liq. Cryst.* **1993**, *13*, 201−212.
(12) Tittarelli, F.; Masson, P.; Skoulios, A. *Liq. Cryst.* **1997**, *22*, 721−726.

10.1021/ja051312a CCC: $30.25

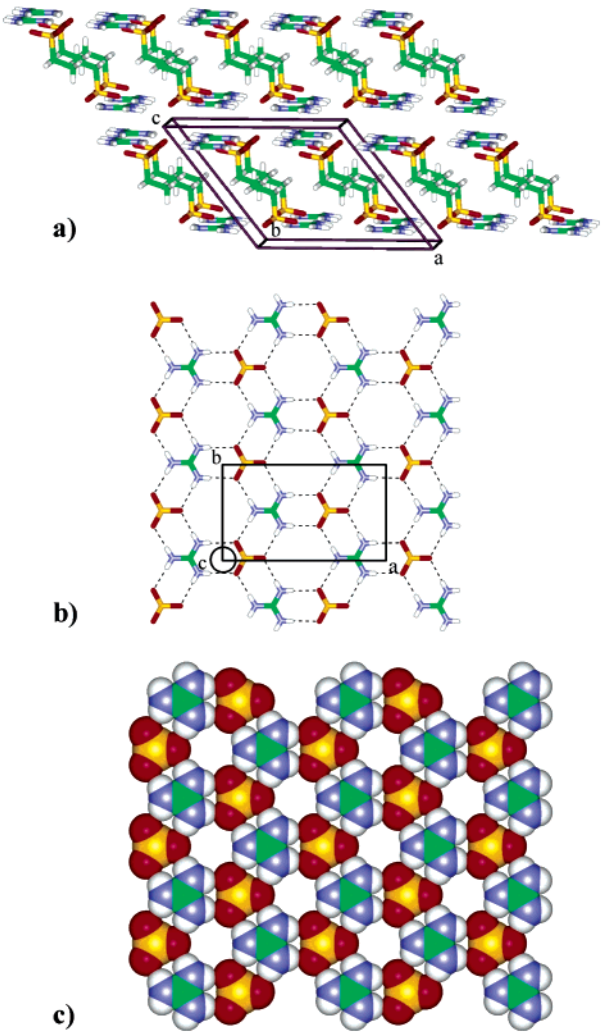

Figure 1. Crystal structure of guanidinium ethanesulfonate drawn by molecular modeling from experimental data of ref 1. (a) Projection on *a*,*c* lattice plane of two layers of molecules; (b) packing mode in *a*,*b* lattice plane of the hydrogen bonded sulfonate and guanidinium ions (a = 12.793 Å, b = 7.398 Å, c = 11.172 Å, β = 128.06°); (c) CPK view of the honeycomb packing of the guanidinium and sulfonate ions. Carbon atoms in green, sulfur in yellow, oxygen in red, hydrogen in white, nitrogen in blue.

ring, the electric charge in the GAS-*n* compounds is concentrated on the oxygen atoms because the alkyl chains are now directly attached to the sulfur atoms; as a result, the ionic interactions are stronger and the overall stability of the supramolecular architecture better secured. This way of tackling the engineering of smectic liquid crystals takes into better account the relations between chemical architecture and crystal or liquid crystal structure.

Results and Discussion

Chemical Synthesis. The GAS-*n* compounds were synthesized as described in the literature,[1,3] by precipitation from solutions of equimolar amounts of guanidine hydrochloride and metal alkanesulfonate:

$$C(NH_2)_3Cl + H(CH_2)_n{-}SO_3M \rightarrow H(CH_2)_n{-}SO_3C(NH_2)_3 + MCl$$

To promote precipitation and ensure purity, special care was taken to select not only the appropriate solvent (pure ethanol for $n \leq 10$ and water/ethanol 1:2 v/v mixture for $n \geq 12$) but also the appropriate metal of the alkanesulfonic salt (silver for $n \leq 10$ and sodium for $n \geq 12$). Not available commercially, the silver alkanesulfonates used were prepared by action of silver nitrate on sodium alkanesulfonates.

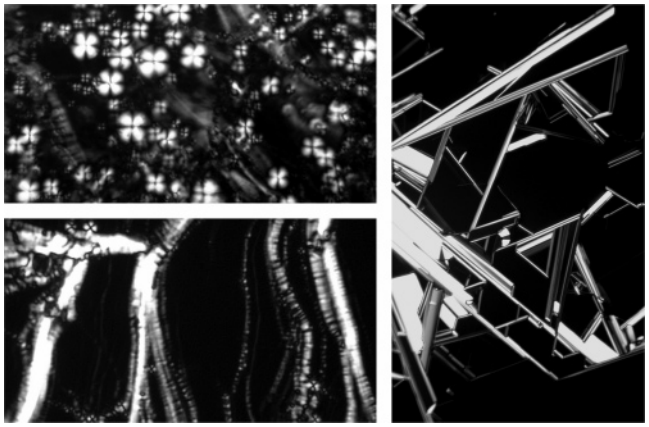

Figure 2. Positive unit and oily streak focal conic textures (left top and bottom) embedded in black homeotropic areas, as observed upon heating GAS-10 to 170 °C. Angular shaped plates of ordered smectic phase (right) grown upon cooling GAS-8 from the isotropic melt to 158 °C.

The chemical structure and purity of the compounds were checked by proton NMR and elemental analysis. Their thermal stability was explored by thermogravimetry. Starting to degrade at about 300 °C when heated at 10 °C min^{-1}, the compounds proved quite stable when maintained at temperatures below 200 °C over periods of time less than a few hours (after 6 h heating at 200 °C, weight losses were smaller than 2.5%).

Optical Microscopy. The thermotropic polymorphic behavior of the GAS-*n* compounds was first approached by polarizing optical microscopy. Occurring as fine white powders at room temperature, these compounds consist of well-defined birefringent hexagonal or trigonal plates similar to those of guanidinium ethanesulfonate crystals of quasi-hexagonal symmetry.[1]

With the exception of GAS-6, which melts directly into an isotropic liquid at 167 °C, the GAS-*n* compounds undergo two sharp transitions as a function of increasing temperature. Taking place at temperatures ranging from 63 °C for GAS-8 to 97 °C for GAS-18 and characterized by a sudden attenuation of the birefringence upon heating, the low-temperature transition corresponds, as established below, to the melting of the crystals into *ordered* smectic phases. Occurring at about 165 °C, the high-temperature transition corresponds either to the melting of the *ordered* smectic phase into an isotropic liquid (GAS-8) or to its conversion into a smectic A phase (GAS-*n*, $10 \leq n \leq 18$). Fairly stable up to 300 °C, the smectic A phases are characterized by typical focal conic textures progressively turning into homeotropic (Figure 2).

On cooling from the smectic A state, the compounds transform back into *ordered* smectic, as shown by the propagation in the optical field of a boundary line sweeping away the focal conic and homeotropic textures and leaving behind opalescent regions discreetly decorated with birefringent points and lines. With GAS-8, the isotropic melt transforms directly into an *ordered* smectic phase, as evidenced by the growth of angularly shaped plates, dark or bright depending upon their orientation in space (perpendicular or parallel to the observation

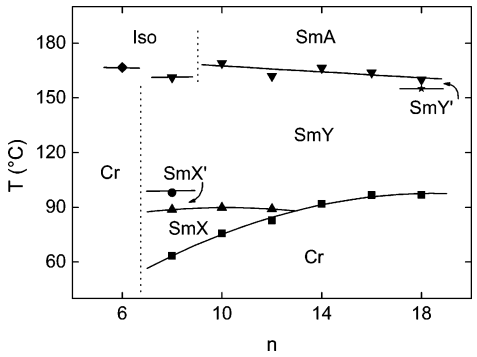

Figure 3. Phase transition temperatures of the GAS-*n* compounds measured on heating by differential scanning calorimetry (onset of endotherms) as a function of the number of carbon atoms in the alkyl chains. (Iso: isotropic liquid; SmA: smectic A phase; Cr: crystal phase; SmX, SmX′, SmY, and SmY′: ordered smectic phases). Transitions involving Iso, SmA, and Cr were confirmed by polarizing optical microscopy.

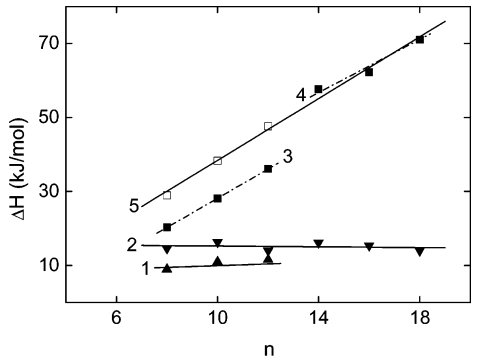

Figure 4. Phase transition enthalpies of the GAS-*n* compounds measured as a function of the chain length by differential scanning calorimetry upon heating. 1: SmX → SmY; 2: SmY → SmA; 3: Cr → SmX; 4: Cr → SmY; 5: Cr → SmX → SmY.

axis) (Figure 2). Worth adding is that the transformation of the *ordered* smectic phases into solid crystals could not be detected visually.

Differential Scanning Calorimetry. The phase diagram of the GAS-*n* compounds was then investigated by differential scanning calorimetry. The thermograms registered upon heating and subsequent cooling in the temperature range from ambient up to 220 °C showed the presence of several sharp peaks indicative of well-defined reversible first-order phase transitions. Only partly detected by optical microscopy, these transitions reveal a rich liquid crystal polymorphism involving a number of *ordered* smectic phases followed at high temperature by a smectic A phase (Figure 3). The transitions induced by cooling proceed, as normally expected, with a certain hysteresis due to nucleation. Unlike the high-temperature transitions between liquid crystalline phases, which take place with virtually no hysteresis, the low-temperature crystallization develops with a delay of as much as 30 °C; this permits the transient formation of additional *ordered* smectic phases (SmX and SmX′), unobserved upon heating and consequently monotropic in nature.

The enthalpy changes involved in these transitions indicate two types of thermal behavior (Figure 4). Independent of the chain length, the enthalpies associated with the SmX → SmY (10 kJ/mol, curve 1) and SmY → SmA (15 kJ/mol, curve 2) transitions are clearly related to the structural rearrangement of the ionic guanidinium sulfonate parts of the molecules. In contrast, strongly dependent upon the chain length, and more-

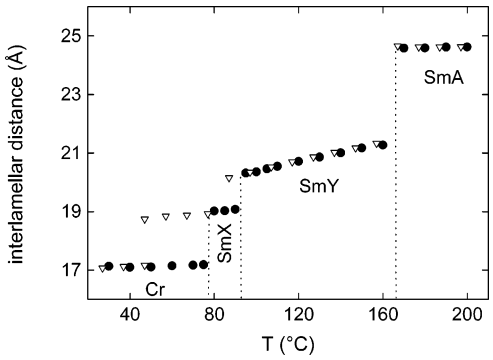

Figure 5. Temperature dependence of the lamellar period of GAS-10 as observed by small-angle X-ray diffraction upon heating (solid circles) and subsequent cooling (empty triangles). Note hysteresis upon cooling.

over, growing linearly with *n*, the enthalpies associated with the Cr → SmX (curve 3) or Cr → SmY (curve 4) phase transitions are unquestionably related to the melting of the alkyl chains. Interestingly enough, the enthalpy changes associated with the conversion of Cr into SmY (curve 5), either measured directly for $14 \leq n \leq 18$, or else calculated for $8 \leq n \leq 12$ by adding up the enthalpies of the Cr → SmX(X′) → SmY transitions, grow linearly with *n* according to the equation (established by a linear least-squares fit of the experimental data, with $R = 0.996$):

$$\Delta H\ (\text{kJ/mol}) = -[3.3 \pm 2.6] + [4.17 \pm 0.20]n$$

The slope of the $\Delta H(n)$ line, which measures the contribution of one methylene group to the melting enthalpy of the alkyl chains, is identical, as normally expected, with that (4.1 kJ/mol) of linear paraffins in the crystalline state.[13] As for the Y-intercept, its negative value is rather small when compared to the energy of the strong Coulombic and hydrogen bonding interactions of the guanidinium and sulfonate ions, suggesting that to gain free energy the ionic groups reorganize themselves slightly.

X-ray Scattering. The polymorphism of the GAS-*n* compounds was next inspected by X-ray scattering. Analyzed in detail, the structure of the crystalline and smectic phases proved to be lamellar in the whole range of temperatures explored (see below). Deduced from the small-angle reflections, the lamellar periods change stepwise with temperature, in agreement with the phase transitions detected previously (Figure 5). On the other hand, the aspect of the X-ray patterns in the wide-angle region permits one to confirm the melting of the alkyl chains and also to catch the unstable character of the monotropic phases mentioned above.

Infrared Spectroscopy. The temperature dependence of the hydrogen bonding of the molecules was then investigated by infrared spectroscopy according to an experimental procedure described recently.[3] A series of spectra were recorded at a series of temperatures ranging from room temperature up to about 200 °C. Special attention was given to the 3000−3600 cm^{-1} absorption region, which contains information about the N−H stretching vibrations related to hydrogen bonding.

Compounds GAS-10 and GAS-14 were found to have the same infrared absorption behavior (Figure 6). At low temper-

(13) Abied, H.; Guillon, D.; Skoulios, A.; Weber, P.; Giroud-Godquin, A.-M.; Marchon, J. C. *Liq. Cryst.* **1987**, *2*, 269−279.

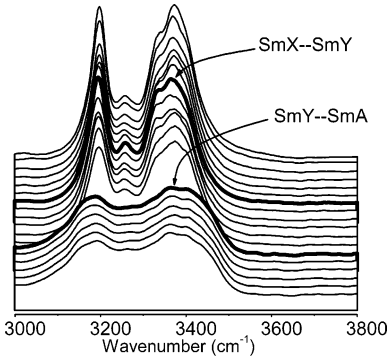

Figure 6. IR absorption spectra of GAS-10 in the 3000−3800 cm^{-1} N−H stretching region, recorded as a function of increasing temperature in the range from 30 °C (upper curve) to 200 °C (lower curve) with steps of 10 °C. The Cr → SmX → SmY → SmA phase transitions, taking place at 76, 90, and 169 °C, were detected by DSC (see Figure 3).

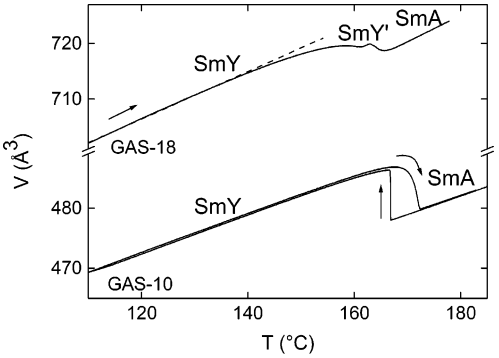

Figure 7. Temperature dependence of the molecular volume of GAS-10 and GAS-18. Note the departure from linearity in the SmY state of GAS-18, below the transition to SmY′.

atures in the crystalline state, the spectra contain four absorption bands (3195, 3253, 3344, and 3389 cm^{-1}, deduced from a least-squares multiple Lorentzian fit of the experimental data) close to those reported in the literature for GAS-2 (3191, 3260, 3334, and 3359 cm^{-1}).[1] The number of these bands indicates the existence of symmetrical and asymmetrical N−H stretching vibrations in an anisotropic environment of the NH_2 groups (due to the relative shift of the ionic sheets in the polar bilayers, Figure 1). The position of the bands is basically independent of temperature (3193, 3257, 3343, and 3395 cm^{-1} in SmY at 120 °C; 3177, 3285, 3367, and 3432 cm^{-1} in SmA at 180 °C), suggesting that the strength of the N−H oscillators is hardly affected by the polymorphic process. Below the SmY → SmA phase transition, the intensity of the absorption bands declines slowly, their width grows weakly, and their total area decays very little with increasing temperature, without measurable disruption at the Cr → SmX → SmY transitions. In contrast, at the SmY → SmA transition, the aspect of the absorption bands changes markedly. Their height decreases, and their width broadens out considerably, indicating a wider distribution of the strength of the N−H oscillators (due to thermal agitation and molecular disordering). Quite interestingly, however, their total area decreases by no more than 15%, suggesting a weak reduction of the number of N−H oscillators.

The infrared absorption behavior of GAS-18 is quite similar, except that the absorption decay, which in the case of GAS-10 and GAS-14 proceeds abruptly at the transition from SmY to SmA, proceeds now progressively between 120 °C (middle of the temperature range of stability of SmY, Figure 3) and 155 °C (upper limit of stability of SmY). This means that the absorption in SmY′ is roughly the same as that in SmA and further suggests that the transition from SmY to SmY′ goes, as confirmed below by X-ray diffraction, through a biphasic region, most likely due to the presence of impurities undetectable by chemical analysis.

Dilatometry. The packing density of the GAS-*n* molecules was subsequently measured by dilatometry for $n = 10$ and 18 in the range from 110 to 190 °C. Figure 7 shows that, in the range of stability of each one of the phases observed, the molecular volume changes slowly with temperature in a perfectly reversible manner, whereas it jumps rapidly (with a small hysteresis on cooling) at the transitions between SmY, SmY′, and SmA.

Important to remark is that, upon heating, the molecular volumes unexpectedly decrease at the phase transitions, instead of increasing as generally observed with liquid crystals,[14] and more generally with condensed matter. Simply due to a breaking of the hydrogen bonding of the molecules, this effect is easy to interpret by analogy with what is known to occur in the melting of water.[15] In the crystalline state, the structure of water is dominated by hydrogen bonding; arranged in hollow hexagonal rings, the molecules are kept at a distance from one another in a low density packing. In the liquid state, on the other hand, the hydrogen bonding is partially (10%) disrupted; the hexagonal rings are partially collapsed and the molecules brought closer together. The situation is exactly the same with the *ordered* smectic phases of the GAS-*n* compounds, in which the hydrogen bonded guanidinium and sulfonate ions are held together, as discussed below, at the nodes of a honeycomb lattice with an empty space in the center of the cells (Figure 1). Of interest to add is that the volume expansion of GAS-18 in the SmY state is slowing down well below 155 °C, the SmY → SmY′ transition temperature measured by DSC, in agreement with the observations of infrared spectroscopy, suggesting the coexistence of the two phases in a wide range of temperatures.

In the range of stability of each one of the phases encountered, the molecular volume grows linearly with temperature (Figure 7) as currently observed with condensed matter, according to the equations (established by a least-squares fit of the experimental data collected upon heating, $R = 0.99997$):

GAS-10 SmY:

$$V(\text{Å}^3) = [433.78 \pm 0.02] + [0.3235 \pm 0.0001]\, T(°\text{C})$$

GAS-10 SmA:

$$V(\text{Å}^3) = [426.48 \pm 0.03] + [0.3084 \pm 0.0002]\, T(°\text{C})$$

GAS-18 SmA:

$$V(\text{Å}^3) = [639.88 \pm 0.03] + [0.4731 \pm 0.0002]\, T(°\text{C})$$

By comparing the molecular volume of GAS-10 and GAS-18 in the smectic A state, it is then possible to calculate the molecular volume of the methylene groups, $V_{CH_2}(\text{Å}^3) = 26.7 + 0.021\, T(°\text{C})$, and thus bring a direct proof of the molten state of the alkyl chains — larger than that calculated for paraffin crystals (23.5 Å^3),[4] the value found is, indeed, identical with

(14) Guillon, D.; Skoulios, A. *Mol. Cryst. Liq. Cryst.* **1977**, *39*, 139−157.
(15) Atkins, P.; de Paula, J. *Physical Chemistry*, 7th ed.; University Press: Oxford, 2002; pp 710 and 789.

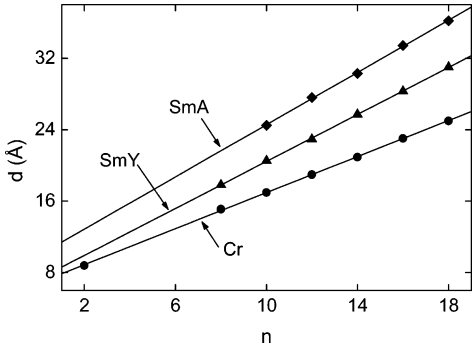

Figure 8. Variation of the lamellar period of the GAS-*n* compounds as a function of the number of carbon atoms in the alkyl chains: Cr at 25 °C, SmY at 120 °C, and SmA at 180 °C.

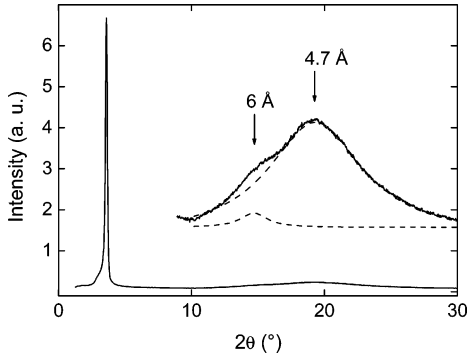

Figure 9. X-ray powder diffraction pattern of GAS-10 in the smectic A state at 180 °C. For clarity, the intensity at Bragg angles at $2\theta > 9°$ is multiplied by 20. Dotted curves represent the intensity distribution of the wide-angle diffuse rings, as determined by a least-squares double Lorentzian fit of the experimental data.

that of paraffins in the liquid state [$V_{CH_2}(Å^3) = 26.6 + 0.020\ T(°C)$].[16] It is further possible to calculate, by interpolation, the molecular volume of the GAS-*n* compounds in the smectic A state:

$$V(Å^3) = V_0 + nV_{CH_2} = 178.2 + 30.38n \text{ at } 180\ °C$$

Structure of the Crystal Phases. The powder X-ray patterns of the GAS-*n* compounds at low temperature consist of a great number of Bragg reflections, all very sharp, indicative of a well-developed three-dimensional crystal lattice. Following one another with reciprocal spacings in the ratio 1:2:3, the reflections located at small angles ($2\theta < 10°$) indicate, as normally observed with long-chained aliphatic derivatives,[4,13,14,17] that the molecules are arranged in a lamellar fashion. The structure corresponds to an alternate superposition of two types of sublayer, made, respectively, of fully stretched alkyl chains and of polar guanidinium sulfonate groups.

Virtually independent of temperature, $(\partial d/\partial T)/d = 1.5 \times 10^{-4}\ K^{-1}$, the period of the lamellar structure, including that of GAS-2 deduced from the crystal lattice parameters ($d_{n=2} = c \times \sin\beta = 8.8$ Å),[1] increases linearly with the number n of carbon atoms in the alkyl chains (Figure 8), according to the equation (least-squares fit, $R = 0.9999$):

$$d(Å) = [7.01 \pm 0.11] + [0.999 \pm 0.009]n$$

Just as in the general case of long-chained aliphatic compounds,[4] this behavior means that the GAS-*n* crystals are characterized by a same molecular area and a same tilt of the chains in the layers, no matter what the chain length. Equal to the thickness deduced by molecular modeling from the crystal structure of GAS-2,[1] the Y-intercept of the $d(n)$ straight line implies that the polar sublayers are made of ions arranged in double layers. Significantly smaller than half the length of one zigzag in a fully extended paraffin chain (1.27 Å),[18] the slope ($m = 0.999$ Å) of the $d(n)$ straight line, which represents the growth rate of the lamellar thickness with the number of methylene groups, implies that the alkyl chains are not only interdigitated to form single layers but also tilted away from the layer normal by an angle as large as $\phi = \cos^{-1}(m/1.27) \cong 38°$. Knowing the cross-sectional area of the alkyl chains in the crystalline state ($\sigma \cong 18.5$ Å^2),[4] it is easy to calculate the area $s = \sigma/\cos\phi \cong 23.5$ Å^2 covered in the layers by one alkyl chain, as well as the area $S = 2s$ covered by one guanidinium sulfonate ion pair. The values found are in harmony with those determined crystallographically for GAS-2 ($s = S/2 = ab/4 = 23.66$ Å^2, Figure 1), for which the ions are assembled according to a quasi-hexagonal ($a \cong b\sqrt{3}$) honeycomb lattice.[1] Such an arrangement is consistent not only with the observations of infrared spectroscopy but also with the results of a recent crystallographic study of long-chained guanidinium alkylbiphenylsulfonates successfully grown in the form of single crystals of good quality.[7]

Structure of the Smectic A Phases. The smectic A structure of the GAS-*n* compounds is identical with that described recently for the guanidinium alkylbenzenesulfonates (GABS-*n*).[3] It consists of an alternate periodic stacking of layers made of alkyl chains and ionic groups, both in a molten state. The X-ray patterns recorded contain two equidistant and sharp small-angle reflections, indicative of a well-developed layering of the molecules (Figure 9). In addition, they contain two diffuse wide-angle rings at 4.7 and 6.0 Å, related to the liquidlike conformation of the alkyl chains and to the disordered arrangement of the ions in the polar sublayers, respectively.

Virtually independent of temperature, $(\partial d/\partial T)/d \cong 6.5 \times 10^{-5}\ K^{-1}$, the smectic period deduced from the small-angle reflections grows linearly with the length of the alkyl chains (Figure 8), according to the equation ($R = 0.9997$):

$$d(Å) = [9.85 \pm 0.29] + [1.463 \pm 0.020]n$$

Contrary to the case of the crystal phases, this linear behavior cannot be interpreted without discussion as a sign of invariance of the molecular area. The reason is simply that, now arranged in a disorderly fashion, the ions may very well spread out in the layers to degrees depending upon the chain length, and actually, when calculated directly from the experimental values of $V(n)$ and $d(n)$, the molecular area $\underline{S}(n) = V(n)/d(n)$, which measures the contribution of one molecule to the lateral spreading of the smectic layers, proves to grow with n, slowly but measurably, with a relative expansion coefficient of $(\partial\underline{S}/\partial n)/\underline{S} \cong 5 \times 10^{-3}$ (Figure 10). Conversely, the thickness $d_0(n) = V_0/\underline{S}(n)$ of the polar sublayers, calculated from the experimental value of the volume of the ionic headgroups, $V_0 = V(n = 0) = 178.2$ Å^3, decreases with increasing n (Figure 10).

(16) Doolittle, A. K. *J. Appl. Phys.* **1951**, *22*, 1471−1475.
(17) Vold, R. D.; Hattiangdi, G. S. *Ind. J. Chem.* **1949**, *41*, 2311−2320.
(18) The lamellar period of the linear paraffins in the orthorhombic crystalline state[4] increases linearly with the number of carbon atoms as $d(Å) = [1.94 \pm 0.33] + [1.270 \pm 0.001]n$.

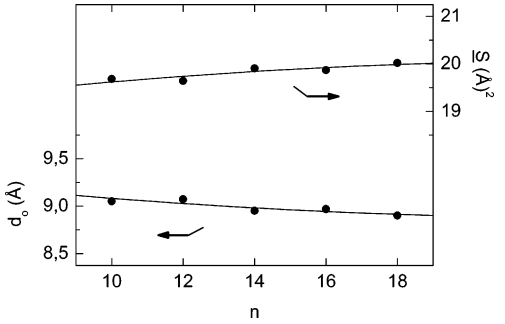

Figure 10. Variation of the molecular area $\underline{S}$ and thickness d_0 of the polar sublayers of the GAS-*n* compounds in the smectic A state at 180 °C as a function of the number of carbon atoms in the alkyl chains.

With the ionic groups facing each other at the surface of the layers, the area $\underline{S}$ corresponds to half the area covered in the layers by one guanidinium sulfonate ion pair ($\underline{S} = S/2$). Its average value ($\underline{S} \cong 20$ Å^2) compares well not only with that ($\underline{S} \cong 21$ Å^2) found recently for the GABS-*n* compounds[3] but also with that ($S/2 \cong (2/\sqrt{3})\ 6^2/2 \cong 20.8$ Å^2) deduced from the diffuse X-ray ring at 6 Å, interpreted as reflecting a local (over roughly 3 unit cells) honeycomb arrangement of the ions in the layers. Of interest to note is that $\underline{S}$ is slightly smaller than expected from the packing of the ions in the crystal ($S/2 = 23.5$ Å^2);[1] this is due of course to the fact that because of the partial disruption of the hydrogen bonding and collapsing of the honeycomb lattice, the ions have come closer together. As for the average value of d_0 (≅9.0 Å), it is significantly larger than that (7.01 Å) measured in the crystal, suggesting that the ions are packed, not in perfect double layers, but in layers somewhat thicker. Probably, in the places where the hydrogen bonds are disrupted, some of the sulfonate ions leave their positions on the honeycomb lattice and, subject to Coulombic interactions, come to sit on top of the guanidinium counterions, out of the bilayers.

Common Features of the Ordered Smectic Y Phases. The GAS-*n* compounds exhibit several *ordered* smectic phases — SmX, SmX′, SmY, and SmY′ — between the low-temperature crystal and the high-temperature smectic A or isotropic liquid. Incapable of surviving long enough, the monotropic SmX and SmX′ phases could not be analyzed properly and were thus left uncharacterized. Having difficulty in reaching equilibrium, the SmY phase of GAS-8 was similarly discarded.

The powder X-ray patterns of the SmY and SmY′ phases contain two or three sharp reflections in the small-angle region, related to the smectic layering of the molecules. Depending very little upon temperature, $(\partial d/\partial T)/d \cong +9 \times 10^{-4}$ K^{-1}, the smectic period *d* of the SmY phases grows linearly with the length of the alkyl chains (Figure 8), according to the equation ($R = 0.9999$):

$$d(\text{Å}) = [7.28 \pm 0.13] + [1.316 \pm 0.010]n$$

Deduced from the Y-intercept of $d(n)$ under the assumption of constant molecular area,[19] the thickness of the polar sublayers ($d_0 = 7.28 \pm 0.13$ Å) is comparable to that (7.01 ± 0.11 Å) found in the crystal, implying that the ionic species are packed in double layers.

(19) This assumption is perfectly legitimate here. As discussed below, the ionic groups are indeed arranged laterally according to a hexagonal lattice whose parameter (7.2 Å) is independent of the chain length.

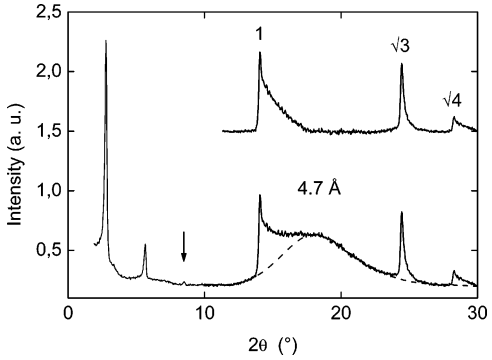

Figure 11. X-ray powder diffraction pattern of GAS-18 in the smectic Y state at 120 °C. Dotted curve represents the intensity distribution of the wide-angle diffuse ring related to the molten alkyl chains, as determined by a least-squares Lorentzian fit of the experimental data. Top right: Intensity distribution of the wide-angle reflections was deduced from the experimental data by subtraction of the diffuse ring.

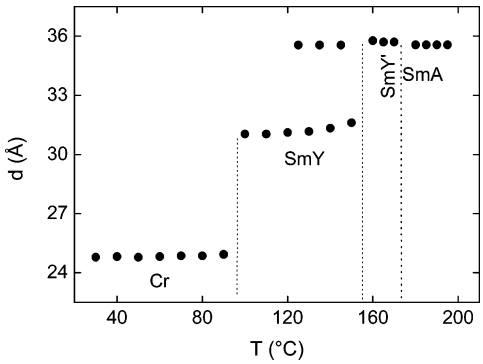

Figure 12. Variation of the lamellar period of GAS-18 upon heating. Vertical lines indicate the phase transition temperatures determined by DSC. Note the coexistence of SmY and SmY′ between 125 and 155 °C.

In addition to a diffuse ring at about 4.7 Å, related to the *molten* state of the alkyl chains, the X-ray patterns contain a certain number of wide-angle reflections related to the lateral arrangement of the ions within the smectic layers and to the stacking mode of these layers in three-dimensional space (Figure 11). Depending crucially upon the chain length, the number and profile of these reflections permit one to identify a series of distinct structures, which will be discussed separately in the following sections. Despite their different characteristics, these structures were, for convenience, all considered to fall into the same class of SmY phases.

Ordered Smectic Structure of GAS-18. The GAS-18 compound exhibits two *ordered* smectic phases, SmY and SmY′, following each other as a function of increasing temperature (Figure 3). Coming immediately after the crystal, the low-temperature SmY phase appears at 97 °C, and preceding SmA, the high-temperature SmY′ phase disappears at 158 °C. As already suggested by infrared spectroscopy and dilatometry, and further confirmed by X-ray diffraction (Figure 12), the transition from SmY to SmY′ is not abrupt but develops through a biphasic region.

In addition to the small-angle reflections related to the smectic layering, the X-ray patterns contain three sharp wide-angle reflections (Figure 11) ranging with reciprocal spacings in the ratio $1{:}\sqrt{3}{:}\sqrt{4}$ and so revealing the existence of a hexagonal two-dimensional crystal lattice. Virtually independent of temperature, $(\partial D/\partial T)/D \cong -5 \times 10^{-5}$ K^{-1}, the hexagonal unit cell parameter, $D = 7.2 \pm 0.05$ Å, is very close to that of the GAS-2

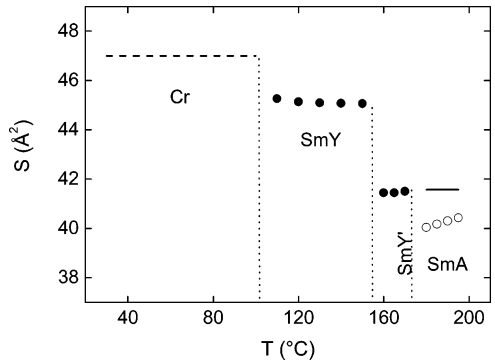

Figure 13. Temperature dependence of the area covered in the layers of GAS-18 by one guanidinium sulfonate group. Vertical dotted lines indicate the phase transition temperatures determined by DSC. Horizontal dashed line is calculated from the area *s* covered in the crystalline layers by every alkyl chain, $S = 2s = 2 \times 23.5 = 47$ Å^2. Solid circles are calculated from the hexagonal unit cell parameter, $S = 2D^2/\sqrt{3}$. Empty circles are calculated by combining the smectic period with the molecular volume, $S = 2V/d$ (number 2 reflects the bilayered arrangement of the ions). Horizontal solid line is deduced from the spacing of the wide-angle diffuse ring, $S = 2 \times 6^2/\sqrt{3} = 41.6$ Å^2 (this value is larger because the wide-angle ring refers mainly to the small ordered regions in which the low-density honeycomb arrangement is preserved).

crystal ($b \cong a/\sqrt{3} \cong 7.39$ Å, Figure 1),[1] strongly suggesting that in both cases the polar bilayers have the same internal structure. These bilayers consist of two ionic sheets, superposed and possibly shifted to some extent with respect to one another,[20] each of them being made of guanidinium and sulfonate ions arranged according to a honeycomb hexagonal lattice (Figure 1). In short, the SmY structure is fundamentally smectic B in symmetry[8] and corresponds to an alternate stacking of layers of molten alkyl chains and of ordered bilayers of guanidinium and sulfonate ions.

Important to stress now is the marked dissymmetry in shape of the wide-angle reflections (Figure 11). The steepness of the small-angle wings is a clear indication that the hexagonal correlations of the ions in the bilayers extend over long distances, actually over 330 Å as deduced from the width of the small-angle wing.[21] As to the stretched profile of the wide-angle wings, it reveals, as well-known in crystallography,[21] the absence of positional register of the smectic layers sliding freely on top of one another.

The X-ray patterns of the high-temperature SmY′ phase are very similar to those of SmY, except that the wide-angle reflections are now somewhat weaker and wider. The corresponding structures are, therefore, pretty much the same, despite certain small differences in their parameters. In the first place, on passing from SmY to SmY′, the correlation length of the hexagonal ordering inside the layers falls from 330 to 200 Å, as shown by the widening of the wide-angle reflections. Then, due to the breaking of 15% of the hydrogen bonds and a partial collapsing of the honeycomb lattice, the molecular area $S = \sqrt{3}D^2/2$ shrinks by 8% (Figure 13), as indicated by the hexagonal unit cell parameter *D* falling from 7.2 to 6.9 Å, and finally, the smectic period *d* increases by 16% (Figure 12) as a result of the contraction of the molecular area at constant molecular volume ($\Delta V/V \cong -0.6\%$).

At the transition from Cr to SmY, the alkyl chains melt abruptly as evidenced by the emergence in the X-ray patterns of a diffuse ring at 4.7 Å, by the rate of growth of the transition enthalpy as a function of the chain length, and by the dramatic increase of molecular volume $S\,d/2$ from 590 to 700 Å^3. In the same time, the ionic groups keep their crystalline arrangement, as proven by infrared spectroscopy and X-ray diffraction. By the way, the decrease of the molecular area from 47 to 45 Å^2 (Figure 13) is simply due to the relaxation of the mechanical constraints imposed upon the ions by the alkyl chains when crystallized.

At the transition from SmY′ to SmA, the ionic species melt as well, as shown by the disappearance in the X-ray patterns of the sharp wide-angle reflections and the emergence of a diffuse ring at 6.0 Å. Quite remarkably, the smectic period and the molecular area are little concerned by the transition (Figures 12 and 13), suggesting that the molecular packing remains roughly unchanged.

To finish, it is useful to question whether, despite their minor differences, the SmY and SmY′ phases are really identical or essentially distinct with regard to their detailed symmetry. With the experimental evidence available, especially in the absence of X-ray diffraction experiments with macroscopically oriented samples, it is extremely difficult to come to a clear conclusion about this matter. It is indeed impossible to decide whether, despite their freedom of gliding over one another, the smectic layers can nevertheless preserve a common orientation about their axis, leading to what is known as an *hexatic* smectic B,[8] or else rotate in their plane, giving rise to a *rotationally disordered* smectic B phase.[22] Plausibly enough, the better ordered low-temperature SmY might very well be hexatic, while the worse ordered high-temperature SmY′ may be rotationally disordered.

Ordered Smectic Structures of GAS-10 and GAS-12. In addition to the diffuse ring at 4.7 Å, which signals the molten state of the alkyl chains, the X-ray patterns of the GAS-10 and GAS-12 compounds in the SmY state contain a great number of sharp wide-angle reflections indicative of a well-developed three-dimensional crystal lattice (Figure 14). Depending upon the thermal history of the samples, these patterns permit one to identify two distinct structures, falling into the category of the so-called *crystalline* smectic phases.[23] For GAS-10, form 1 is obtained exclusively by heating fresh (never heated before) crystalline samples, while form 2 is obtained either by cooling smectic A or by heating samples after recrystallization. For GAS-12, form 1 is obtained as described previously, by heating fresh crystals, but also by cooling smectic A samples (never cooled before); on the other hand, form 2 is systematically obtained in all subsequent heating and cooling cycles. It is interesting to add that both forms do not change isothermally with time, even after annealing at 150 °C for 15 days, and yet at least one of them should be thermodynamically metastable.

To determine the main features of the two forms of SmY, it is necessary, at least, to establish their crystal lattices. After several attempts, the indexing of all the reflections could be

(20) The relative shift of the ionic sheets in the polar bilayers of SmY is impossible to measure experimentally by X-ray diffraction. It is also impossible to evaluate through molecular modeling by minimizing the electrostatic interactions because the electron density distribution in the ionic sheets is strongly dependent upon the relative shift.

(21) Guinier, A. *Théorie et Technique de la Radiocristallographie*; Dunod: Paris, 1956.

(22) Tsiourvas, D.; Paleos, C.M.; Skoulios, A. *Macromolecules* **1997**, *30*, 7191−7195.

(23) Pershan, P. S. *Structure of Liquid Crystal Phases*; World Scientific Lecture Notes in Physics; World Scientific Publishing: Singapore, 1988; p 23.

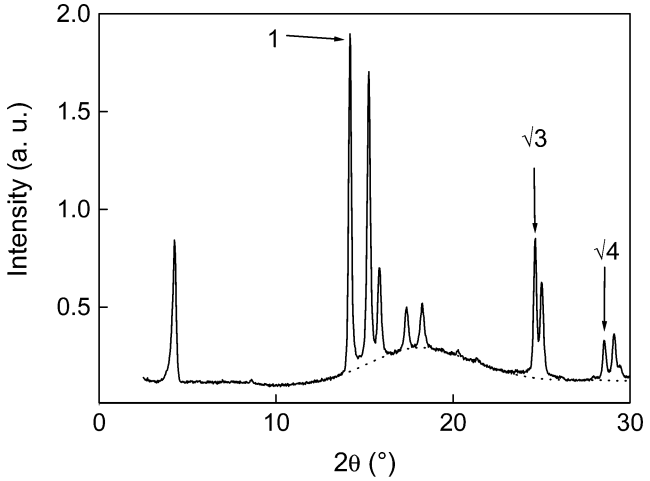

Figure 14. X-ray powder diffraction pattern of form 1 of GAS-10 in the smectic Y state at 120 °C. Dotted line represents the diffuse scattering of the molten alkyl chains.

Table 1. Parameters of the Monoclinic Form 1 and Triclinic Form 2 Lattices of GAS-10 and GAS-12 in the SmY State at 120 °C

	GAS-10	GAS-12
monoclinic	$a = 12.57 \pm 0.04$ Å	$a = 12.58 \pm 0.04$ Å
	$b = 7.22 \pm 0.02$ Å	$b = 7.23 \pm 0.02$ Å
	$c = 20.59 \pm 0.14$ Å	$c = 23.06 \pm 0.16$ Å
	$\beta = 95.89 \pm 0.10°$	$\beta = 95.44 \pm 0.10°$
	$V_{cell} = 1860 \pm 24$ Å^3	$V_{cell} = 2088 \pm 26$ Å^3
triclinic	$a = 12.61 \pm 0.04$ Å	$a = 12.62 \pm 0.04$ Å
	$b = 7.24 \pm 0.02$ Å	$b = 7.25 \pm 0.02$ Å
	$c = 41.18 \pm 0.30$ Å	$c = 46.21 \pm 0.32$ Å
	$\alpha = 93.36 \pm 0.06°$	$\alpha = 93.22 \pm 0.06°$
	$\beta = 95.86 \pm 0.10°$	$\beta = 95.58 \pm 0.10°$
	$\gamma = 90°$	$\gamma = 90°$
	$V_{cell} = 3734 \pm 50$ Å^3	$V_{cell} = 420 \pm 54$ Å^3

achieved thanks to the following observations. First, the period of the lamellar structure deduced from the small-angle reflections compares well with the full length of the molecules. As usually done with long-chained aliphatic compounds,[4] the small-angle reflections were thus indexed as *00l*. Second, part of the wide-angle reflections, distinctly stronger than the others, are located at Bragg angles independent of the chain length. Obviously related to the lateral packing of the molecules in the layers, they were indexed as reflections *hk0*. With reciprocal spacings ranging as $1:\sqrt{3}:\sqrt{4}$, these reflections indicate the existence of a hexagonal two-dimensional crystal lattice. Finally, all the other wide-angle reflections flock together in separate groups, each one associated with a particular *hk0* reflection (Figure 14). With reciprocal spacings depending on the chain length, these reflections correspond to crystalline periodicities along directions away from the layer normals. They were indexed as reflections *hkl*. With these observations in mind, the X-ray patterns of GAS-10 and GAS-12 were then indexed easily, using standard least-squares computing methods. For simplicity, the lattices determined were arbitrarily described as being monoclinic for form 1 and triclinic for form 2, both having centered rectangular bases and cell parameters ($a/b \equiv \sqrt{3}$) fitting the hexagonal two-dimensional packing of the molecules in the layers (Table 1).

Close inspection of these results leads to the following discussion. The *a* and *b* unit cell vectors of forms 1 or 2 of GAS-10 and GAS-12 define a two-dimensional hexagonal lattice whose parameter ($b \cong 7.24$ Å) is identical with that ($D = 7.2$ Å) of GAS-18. This is a clear indication that the lateral arrangement of the molecules in the smectic layers proceeds in all three compounds according to a same honeycomb hexagonal crystal lattice. The only difference between the observed structures lies in the stacking register of the ionic bilayers. These either slide freely on top of one another as observed with GAS-18 or are locked in well-defined positions according to a three-dimensional monoclinic or triclinic crystal lattice as observed with GAS-10 and GAS-12. Incidentally, the triclinic cell contains two ionic bilayers ($c \times \sin\alpha \times \sin\beta = 2d$, where *d* is the smectic period), while the monoclinic cell contains only one bilayer ($c \times \sin\alpha = d$). It should certainly be of great interest to understand why the ionic bilayers are arranged in such different ways, but the electrostatic interactions of the layers are very difficult to handle realistically in computer simulations.[20]

Finally, the structural parameters of forms 1 and 2 were studied as a function of temperature between 95 and 155 °C. While the relative thermal expansion coefficient of the thickness of the smectic layers is rather large, $(\partial c/\partial T)/c \cong +8.2 \times 10^{-4}$ K^{-1}, that of the cell parameters related to the lateral packing of the molecules is in contrast very small, $(\partial a,b/\partial T)/a,b \cong -0.3 \times 10^{-4}$ K^{-1}. This is in harmony with the fact that the alkyl chains are molten and the polar sublayers crystalline. As for the temperature dependence of the angular cell parameters, it is nearly zero, $(\partial\beta/\partial T)/\beta \cong -5 \times 10^{-5}$ K^{-1} for the monoclinic, and $(\partial\beta/\partial T)/\beta \cong -5 \times 10^{-7}$ K^{-1} and $(\partial\alpha/\partial T)/\alpha \cong -6 \times 10^{-8}$ K^{-1} for the triclinic lattices. Finally, the thermal expansion coefficient of the unit cell volume, $(\partial V/\partial T)/V \cong +7.6 \times 10^{-4}$ K^{-1}, compares well with that of the molecular volume of ordinary organic liquids. Note by the way that the molecular volume of GAS-10 ($V = 466 \pm 6$ Å^3), deduced from the cell parameters of the monoclinic and triclinic crystal lattices at 120 °C, is in agreement with that ($V = 473 \pm 1$ Å^3) measured directly by dilatometry.

Ordered Smectic Structure of GAS-14 and GAS-16. The aspect of the X-ray patterns of GAS-14 and GAS-16 in the SmY state is intermediate between those of GAS-10 and GAS-18 (Figure 15). With a Bragg spacing equal to that of GAS-18, the sharp *hk0* reflections observed with GAS-10 and GAS-12 subsist in GAS-14 and GAS-16, indicating that the molecules continue to be packed in the same way, according to a same hexagonal lattice ($D = 7.2$ Å), no matter what the chain length. On the other hand, the *hkl* ($l \neq 0$) reflections, whose spacings depend on the chain length, actually subsist in GAS-14 and GAS-16, but clearly widen out and weaken in intensity until they finally merge into the stretched outer wing of the wide-angle reflections of GAS-18 (Figure 15). Planar disorder sets up, therefore, among the smectic layers,[21] obviously due to the fact that the positional correlations of the smectic layers fade out progressively when the spacing of the ionic sublayers grows.

Conclusions

The main result of the present work is to have obtained an *ordered* smectic (SmY) phase between the low-temperature crystal (Cr) and the high-temperature smectic A (SmA), and more importantly, to have shown that, in SmY, the guanidinium and sulfonate ions are indeed arranged periodically, according to a hexagonal lattice perfectly consistent with the known honeycomb supramolecular architecture of guanidinium sulfonates.[1] This was further confirmed by infrared spectroscopy,

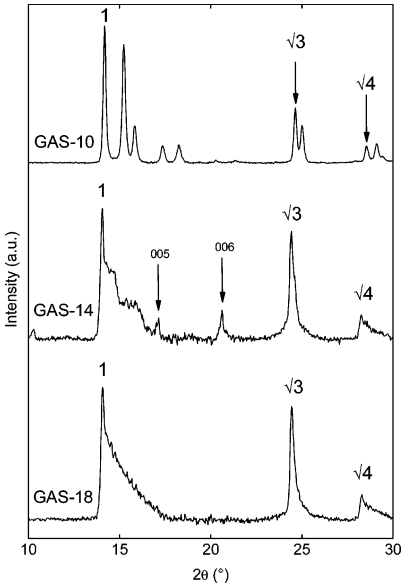

Figure 15. Wide-angle region of the X-ray powder diffraction patterns of GAS-10 (form 1), GAS-14, and GAS-18 in the smectic Y state at 120 °C, calculated by subtraction of the diffuse ring due to the molten alkyl chains (see dotted curves in Figures 11 and 14). Higher order reflections noted as *005* and *006* correspond to the smectic layering of the molecules

which showed the hydrogen bonding to survive at high temperature, almost intact in SmY and only moderately damaged in SmA.

Another result is to have established the detailed structure of the various polymorphic phases observed as a function of increasing temperature. Generically, all these phases have a similar lamellar structure, resulting from an alternate stacking of layers of alkyl chains and guanidinium sulfonate ion pairs. Yet, they differ in several respects, particularly in the physical state of the ions and alkyl chains inside the layers. For instance, the alkyl chains are crystallized in the crystal and molten in the smectic phases, while the ionic groups are molten in the *disordered* smectic A and crystallized in the crystal and *ordered* smectic phases. Such mesophase transformation due to a step-by-step melting of the constituent parts in the molecules has already been reported in the literature, in papers dealing, for instance, with the structural behavior at high temperature of sodium soaps,[5] dodecyle polyglutamate,[24] or polypetides with mesogenic side chains.[25] The range of the in-layer ordering of the molecules extends to infinity in the crystal, to about 300 Å (several tens of unit cells) in the *ordered* SmY, and only to 20 Å (about three unit cells) in the *disordered* SmA phase. Quite interestingly, the degree of hydrogen bonding does not decrease in the same proportion, hardly coming down to 75%.

An additional result, related to the crystallographic structure of the phases encountered, deals specifically with the stacking mode of the lamellae on top of each other. In the crystal phases, the layers of ions and alkyl chains are alternately superposed in perfect crystallographic register. Since both are *crystallized*, they must necessarily have internal structures that are compatible with one another and describable by a same two-dimensional crystal lattice. This is why, in the crystal structures described in the literature,[1,7] the in-layer packing of the ions is not strictly hexagonal as required by the symmetry of the guanidinium and sulfonate ions, and also why the ionic layers are not strictly planar but puckered to some degree. In the *ordered* smectic Y phases, in which the alkyl chains are in a molten state, the crystalline packing of the ions recovers its best hexagonal symmetry. The various SmY structures observed are specifically related to the stacking modes and positional correlations of the ionic layers. In the short-chained GAS-10 and GAS-12, the ionic layers are subject to strong Coulombic forces because of their short separation and so locked in well-defined positions according to a three-dimensional crystal lattice. In contrast, in the long-chained GAS-18, the ionic layers are subject to weak Coulombic forces and so can slide freely on top of each other. In the intermediate case of GAS-14 and GAS-16, the ionic layers are neither bound to superpose in perfect positional register nor totally free to slide over one another, but superposed according to three-dimensional crystal lattices planarly disordered to some extent.

Acknowledgment. The authors wish to thank Dr. B. Heinrich for skilled assistance and helpful discussions in the dilatometry experiments and in the indexation of the powder X-ray patterns corresponding to the three-dimensional crystal lattices found.

Supporting Information Available: Experimental details. This material is available free of charge via the Internet at http://pubs.acs.org.

JA051312A

(24) Thierry, A.; Skoulios, A.; Lang, G.; Forestier, S. *Mol. Cryst. Liq. Cryst.* **1978**, *41*, 125−128.
(25) Watanabe, J.; Tominaga, T. *Macromolecules* **1993**, *26*, 4032−4036.